Biomedical Optics EXPRESS

A wide field-of-view scanning endoscope for whole anal canal imaging

Chao Han,[1,4,5] Jiangtao Huangfu,[1,2,4,6] Lily L. Lai,[3,4,*] and Changhuei Yang[1]

[1] *Electrical Engineering, California Institute of Technology, Pasadena, CA 91125, USA*
[2] *Department of Information and Electronic Engineering, Zhejiang University, Hangzhou 310027, China*
[3] *Division of Surgical Oncology, Department of Surgery, City of Hope, Duarte, CA 91010, USA*
[4] *These authors contributed equally*
[5] *chan@caltech.edu*
[6] *huangfujt@zju.edu.cn*
[*] *llai@coh.org*

Abstract: We report a novel wide field-of-view (FOV) scanning endoscope, the AnCam, which is based on contact image sensor (CIS) technology used in commercialized business card scanners. The AnCam can capture the whole image of the anal canal within 10 seconds with a resolution of 89 μm, a maximum FOV of 100 mm × 120 mm, and a depth-of-field (DOF) of 0.65 mm at 5.9 line pairs per mm (lp/mm). We demonstrate the performance of the AnCam by imaging the entire anal canal of pigs and tracking the dynamics of acetowhite testing. We believe the AnCam can potentially be a simple and convenient solution for screening of the anal canal for dysplasia and for surveillance in patients following treatment for anal cancer.

OCIS codes: (120.4820) Optical systems; (170.2150) Endoscopic imaging; (170.2680) Gastrointestinal.

References and links

1. L. G. Johnson, M. M. Madeleine, L. M. Newcomer, S. M. Schwartz, and J. R. Daling, "Anal cancer incidence and survival: The surveillance, epidemiology, and end results experience, 1973-2000," Cancer **101**(2), 281–288 (2004).
2. R. A. Nelson, A. M. Levine, L. Bernstein, D. D. Smith, and L. L. Lai, "Changing Patterns of Anal Canal Carcinoma in the United States," J. Clin. Oncol. **31**(12), 1569–1575 (2013).
3. M. Frisch, B. Glimelius, A. J. van den Brule, J. Wohlfahrt, C. J. Meijer, J. M. Walboomers, S. Goldman, C. Svensson, H. O. Adami, and M. Melbye, "Sexually transmitted infection as a cause of anal cancer," N. Engl. J. Med. **337**(19), 1350–1358 (1997).
4. C. E. Pineda, J. M. Berry, N. Jay, J. M. Palefsky, and M. L. Welton, "High resolution anoscopy in the planned staged treatment of anal squamous intraepithelial lesions in HIV-negative patients," J. Gastrointest. Surg. **11**(11), 1410–1416 (2007).
5. I. Tramujas da Costa e Silva, L. C. de Lima Ferreira, F. Santos Gimenez, R. A. Gonçalves Guimarães, L. Botinelly Fujimoto, C. R. Barbosa Cabral, R. Venturim Mozzer, and L. de Souza Atala, "High-resolution anoscopy in the diagnosis of anal cancer precursor lesions in renal graft recipients," Ann. Surg. Oncol. **15**(5), 1470–1475 (2008).
6. N. Jay, J. M. Berry, C. J. Hogeboom, E. A. Holly, T. M. Darragh, and J. M. Palefsky, "Colposcopic appearance of anal squamous intraepithelial lesions: relationship to histopathology," Dis. Colon Rectum **40**(8), 919–928 (1997).
7. T. J. Wilkin, S. Palmer, K. F. Brudney, M. A. Chiasson, and T. C. Wright, "Anal intraepithelial neoplasia in heterosexual and homosexual HIV-positive men with access to antiretroviral therapy," J. Infect. Dis. **190**(9), 1685–1691 (2004).
8. G. A. Zheng, X. Z. Ou, and C. H. Yang, "0.5 gigapixel microscopy using a flatbed scanner," Biomed. Opt. Express **5**(1), 1–8 (2014).
9. Z. Göröcs, Y. Y. Ling, M. D. Yu, D. Karahalios, K. Mogharabi, K. Lu, Q. S. Wei, and A. Ozcan, "Giga-pixel fluorescent imaging over an ultra-large field-of-view using a flatbed scanner," Lab Chip **13**(22), 4460–4466 (2013).
10. B. Kumar and S. Gupta, "The acetowhite test in genital human papillomavirus infection in men: what does it add?" J. Eur. Acad. Dermatol. Venereol. **15**(1), 27–29 (2001).

#226184 - $15.00 USD Received 6 Nov 2014; revised 19 Jan 2015; accepted 22 Jan 2015; published 27 Jan 2015

1. Introduction

Anal cancer is a malignancy of the epithelium of the anal canal [1]. As a malignancy that is associated with human papilloma virus (HPV) infection, the incidence of anal canal cancer has increased markedly over the last two decades [2,3]. Although screening for anal cancer results in early detection, screening of at-risk populations has not been widely adopted. The current gold standard for anal cancer screening is high resolution anoscopy (HRA), a technique adapted from standard cervical examination protocols [4–7]. In brief, the procedure is conducted as follows: 3–5% acetic acid is applied, using a soaked gauze, into the anal canal for at least one minute. The gauze is removed and a clear plastic anoscope is passed into the anal canal to retract soft tissues away and to allow the anal mucosa to be evaluated. The colposcope is positioned and used to identify abnormal areas delineated by acetic acid and labeled as "acetowhite" areas. These areas are biopsied to obtain a histological confirmation of the abnormality. A handwritten map and photographs of abnormal areas document the location, appearance, and clinical impression of the biopsied areas.

Although HRA is the current standard examination used to screen for anal cancer, the technique has significant limitations. A typical colposcope has an adjustable magnification of 3 × –17 × with a 13–84-mm diameter FOV (Olympus OCS-3). However, the geometry of the anal canal allows the colposcope to only view small areas of the anal canal at any given time. To complete the entire examination, the colposcope would have to be moved and refocused multiple times. In addition, the ability to identify abnormal from normal tissues is dependent on the skill level of the practitioner and the number of biopsies taken during the examination. Lastly, the exam is charted manually. Digital photographs of areas of concern are highly desirable for serial follow-up but are logistically difficult to implement well. Taken together, the entire procedure is time consuming with an average of more than 30 minutes per exam, requires multiple steps in its set up and execution, depends on the skill set of the provider to identify abnormal areas requiring biopsies, and demands high levels of histopathologic resources for support. A simpler, cheaper, and better alternative for imaging the anal canal for screening purposes is needed.

In recent years, contact image sensor (CIS) technology has been widely used within commercialized flatbed scanners and business card scanners, where a SELFOC lens array (SLA) is used to create a 1:1 image of the document onto a linear image sensor. Recently, CIS has been explored as a low cost solution for wide FOV biomedical imaging [8,9]. Zheng, *et al.* built a wide FOV brightfield scanning microscopy system based on a closed-circuit television (CCTV) lens for image magnification and a flatbed scanner for image acquisition [8]. Göröcs, *et al.* achieved wide FOV fluorescence imaging by adding an excitation light source and an emission filter to the flatbed scanner [9].

Here, we describe a novel anal imaging device developed by adapting a CIS that is disassembled from a low-cost business card scanner for imaging of cylindrical inner surfaces such as the anal canal. We have named this device the AnCam, and describe its setup in detail and establish its resolution and DOF performance. In addition, we report a series of animal model experiments comparing the images of the AnCam with the conventional colposcope in the evaluation of the anal canal. Finally, we demonstrate the use of the AnCam in time-lapse imaging of acetic acid-induced changes of the anal canal to show the dynamic changes resulting from the use of acetic acid on the epithelium as well as the reproducibility of the serial images. To our knowledge, this is the first report of an imaging device for capturing the circumferential inner cylindrical surface of the anal canal.

2. System setup

System setup for the AnCam is shown in Fig. 1, and its basic imaging principle is illustrated in Fig. 1(a). The imaging module consists of a light source, an SLA, and a linear image sensor. The light source contains red, green, and blue (RGB) light-emitting diodes (LEDs)

#226184 - $15.00 USD Received 6 Nov 2014; revised 19 Jan 2015; accepted 22 Jan 2015; published 27 Jan 2015

coupled to a light guide, which provides uniform illumination along its entire length. The SLA is a linear collection of cylindrical lenses (GRIN lenses) (Fig. 1(b)). The light source illuminates the sample of interest, and the SLA is capable of performing good 1:1 imaging (without magnification) and of projecting a strip segment of the sample onto the linear image sensor. In order to obtain an image of the anal canal, which has a cylindrical surface, we incorporated the imaging module into a transparent tube, and carefully realigned the SLA and linear image sensor to fit the geometry of the tube and to ensure the sample on the outer surface of the tube is imaged correctly onto the image sensor. At each step, the imaging module collects one line of image information under three color channel illumination. Via the rotational scan of the imaging module at a constant speed for 360° inside the polycarbonate tube, we obtain a 2D RGB image of the sample throughout the tube surface.

Our AnCam system design and prototype are shown in Fig. 1(c) and 1(d), respectively. The imaging module was directly modified from a CIS that was disassembled from a palm-sized business card scanner (Opticard 821, Plustek). All of the components of the imaging module were then realigned and mounted onto an axis, and fixed inside a polycarbonate tube with a 38.1-mm outer diameter. The holders for the imaging module and the tip of the tube were all made of polylactide (PLA) and fabricated by a 3D printer (MakerBot Replicator 2). The axis was connected to a geared stepper motor (28BYJ-48, Kootek), which was controlled by a microcontroller (Arduino UNO) with a motor shield. The imaging module was driven by the card scanner's own software for LED illumination and image capture, and the rotational speed of the motor was set at 0.68 rad/sec to be synchronized with image acquisition. The noise from the linear image sensor was removed by taking the fast Fourier transform (FFT) of the scanned image then suppressing its abnormal frequency components (in MATLAB).

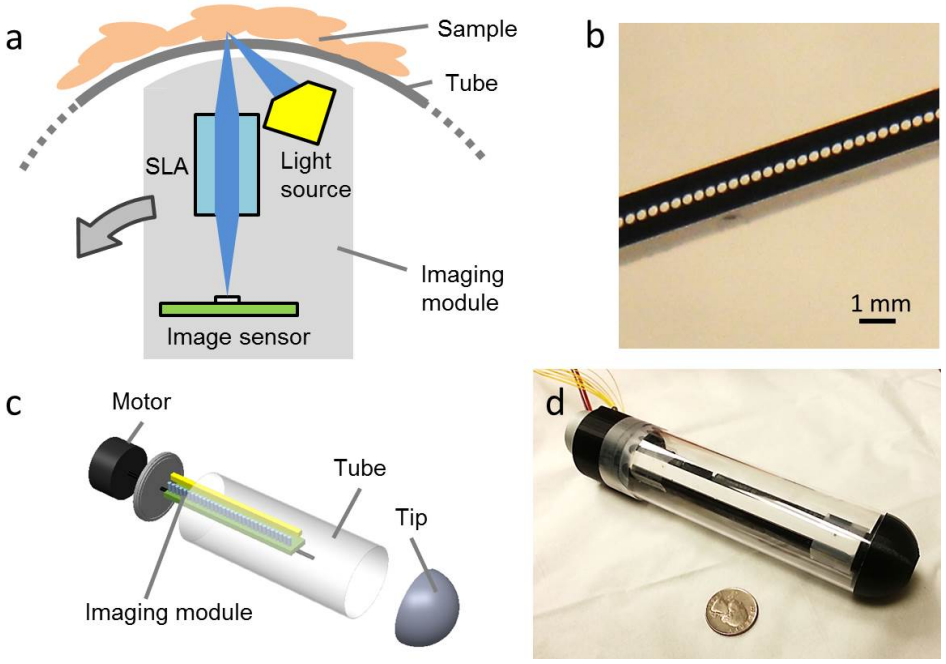

Fig. 1. System setup. (a) The imaging principle of the AnCam. (b) The SELFOC® lens array (SLA) inside the imaging module of the AnCam. (c) The design of the AnCam. (d) A prototype of the AnCam.

#226184 - $15.00 USD Received 6 Nov 2014; revised 19 Jan 2015; accepted 22 Jan 2015; published 27 Jan 2015

3. Results

3.1 Resolution

To verify the resolution of our AnCam, we printed Groups 0–3 of the 1951 USAF resolution target on a transparency film (CAS/Art Services, Inc.) and attached it onto the tube surface for scanning (Fig. 2). The scan was performed along the y direction. As shown in Fig. 2(b)–2(d), the element with 11.3 line pairs per mm (lp/mm, corresponding to 88.5-μm line spacing) is the smallest discernible element; therefore, we can establish a resolution of 89 μm. This resolution is consistent with the image sensor's Nyquist sampling limit of 85 μm, considering that the pixel pitch for the sensor is 42.3 μm (600 dpi). The line visibility in the collected images and the close fit of the observed AnCam resolution to the Nyquist resolution limit suggests that the sensor pixel pitch, rather than the optical imaging scheme, was the resolution-limiting factor in our sample. In other words, the AnCam would likely be able to achieve a finer resolution if the sensor were to be replaced with one of a denser pixel pitch.

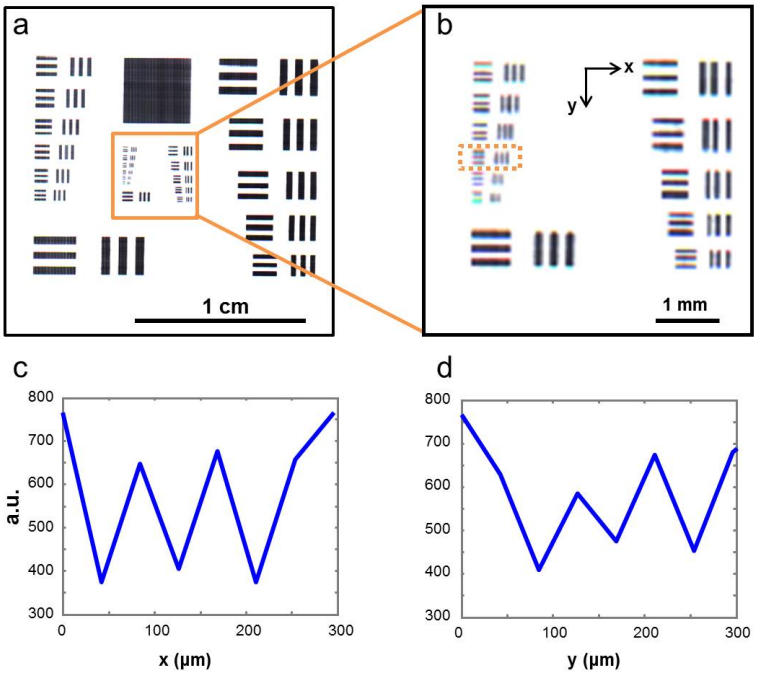

Fig. 2. Resolution test. (a) The image of a resolution target obtained by the AnCam. (b) A zoomed-in region of (a), showing that the 11.3 lp/mm (88.5-μm line spacing) element is discernible (labeled in the orange rectangle). (c-d) The intensity profile of the 11.3-lp/mm element in the x (c) and y (d) directions after summing the red, green, and blue (RGB) channels.

3.2 Depth-of-field

We characterized the DOF of the AnCam to demonstrate its tolerance of tissue unevenness. The DOF measurement is illustrated in Fig. 3. The imaging module was raised by 0.7 mm to make sure that the focal plane of the SLA is above the tube surface. Then a resolution target with a 5.9-lp/mm (170-μm line spacing) line pattern was attached to the tube surface with a tilting angle of $\theta = 1/15$ rad (Fig. 3(a)). The light source of the imaging module was disabled and an external light source was used to provide a uniform illumination onto the target. After obtaining the scanned image (Fig. 3(c)), the modulation transfer function (MTF) at different separation distances was defined as the normalized contrast of the line pattern, and the result was plotted (Fig. 3(b)). The DOF was then defined as the depth range where the MTF was

#226184 - $15.00 USD Received 6 Nov 2014; revised 19 Jan 2015; accepted 22 Jan 2015; published 27 Jan 2015

above 50%, which was calculated to be 0.65 mm at 5.9 lp/mm. Figure 3(d)–3(h) shows representative images of the line pattern at different distances below (Fig. 3(d), 3(e)), at (Fig. 3(f)), and above (Fig. 3(g), 3(h)) the focal plane. Their positions are also marked in Fig. 3(b).

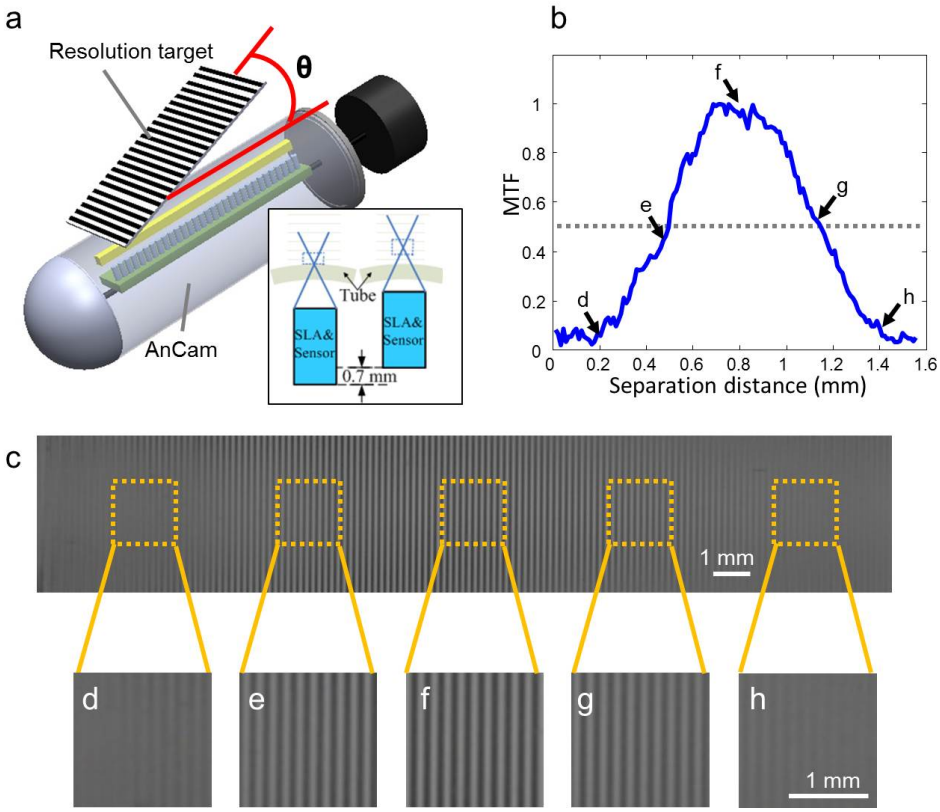

Fig. 3. The depth-of-field (DOF) measurement. (a) The setup for the DOF measurement. A resolution target with a 5.9-lp/mm line pattern was attached on the tube surface of the AnCam at an angle of θ = 1/15 rad. The imaging module was raised by 0.7 mm to make sure the focal plane of the SLA is above the tube surface (bottom-right image). (b) The measured modulation transfer function (MTF) corresponding to the separation distance of the line pattern. (c-h) The scanned image of the target and the zoom-in images of the line pattern with a distance of 0.2 mm (d), 0.5 mm (e), 0.8 mm (f), 1.1 mm (g), and 1.4 mm (d) to the tube surface.

3.3 Entire anal canal imaging using the AnCam in comparison to a colposcope

Next, we compared the performance of the AnCam with that of a conventional colposcope in the imaging of the anal canal. These studies were completed in an *in vivo* pig model. After the pig was anesthetized as per approved institutional protocols, a small region of the anal canal was stained using a marker pen. The AnCam was gently inserted into the anal canal after applying a small amount of water-based lubrication to the top of the device (Fig. 4(a)). The entire cylindrical surface of the anal canal was imaged with a single scan (Fig. 4b). Results of the comparison are shown in Fig. 4(c)–4(e). The image has a FOV of 55 mm × 120 mm (Fig. 4(c)). The stained patterns made from the marker pen are discernible (Fig. 4(d), 4(e)). As a comparison, the same area of the anal canal was examined using a plastic anoscope and a standard colposcope (Olympus OCS-3) with 12 × magnification (Fig. 4(f), 4(g)), and the image was captured using an iPhone 4S camera connected to the eyepiece via a customized adaptor. The yellow and blue arrows in Fig. 4(e) and 4(g) are pointing at the same stained spots viewed under the two systems, as marked by the pen. Both the AnCam and the colposcope can resolve these stained spots. It is also worth noting that the colposcope images

#226184 - $15.00 USD Received 6 Nov 2014; revised 19 Jan 2015; accepted 22 Jan 2015; published 27 Jan 2015

(Fig. 4(f), 4(g)) have unavoidable reflections on the tissue surface due to the illumination of the light source affecting visualization of the anal mucosa.

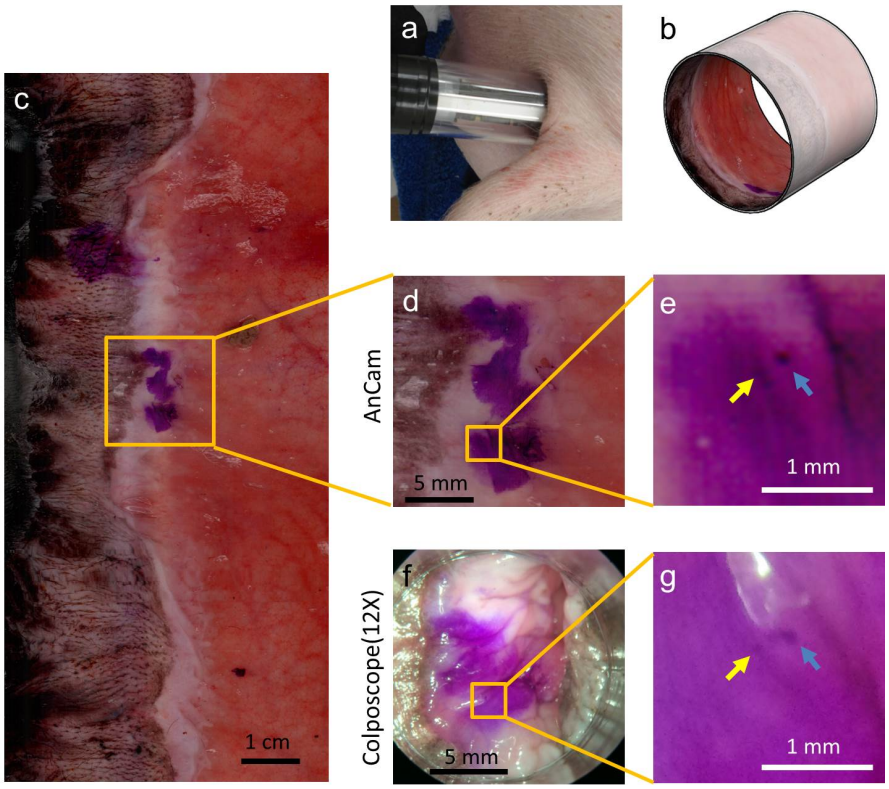

Fig. 4. Whole anal canal imaging. (a) The AnCam was inserted into the anus of a live pig for imaging. (b) The cylindrical surface containing the whole anal canal was imaged with a single scan. (c–e) The wide field-of-view (FOV) image captured by the AnCam (c) with the stained region zoomed in (d,e). (f–g) The same stained region captured by a standard colposcope with 12 × magnification (f) with a zoomed-in and 90°-rotated image (g). The yellow and blue arrows in (e) and (g) are pointing at the same stained spots.

3.4 Time-lapse imaging of acetic acid

Delineation of acetowhite tissues is a critical step in standard HRA and requires application of acetic acid to dehydrate anal mucosa cells. Acetic acid-induced changes of the epithelial surface localize abnormal areas that require biopsy [6,10]. To demonstrate that the AnCam is capable of depicting the dynamic changes in the anal mucosa with serial acetic acid application and of localizing acetowhite areas, we performed acetic acid testing in a live, anesthetized pig. First, we documented the appearance of the anal canal before acetic acid staining (Fig. 5(a), 5(b)). Then, a 5% acetic acid-soaked gauze was inserted into the anal canal for 5 minutes. The gauze was removed, and an AnCam image was obtained (Fig. 5(c)). We repeated the application of acetic acid three times, removed the gauze, reinserted the AnCam, and obtained serial time-lapse images of the anal canal (Fig. 5(c)–5(e)). We compared the entire anal canal before application of acetic acid with the post-acetic acid images, and an area of interest before and after the three rounds of acetic acid staining is shown in Fig. 5(b)–5(e). There was a significant whitening of the anal canal epithelium (yellow arrows) and rectal epithelium (white arrow) after each of the first two stainings (Fig. 5(b)–5(d)). However, there was no further change after the third staining (Fig. 5(e)), arguing that there is no further improvement in acetowhite effect after 10 minutes of acetic acid application. In each of the

#226184 - $15.00 USD Received 6 Nov 2014; revised 19 Jan 2015; accepted 22 Jan 2015; published 27 Jan 2015

images (Fig. 5(b)–5(e)), the anatomic structure of interest was reproduced and comparable. The consistency of the images argues for the potential use of this device in longitudinal follow-up of patients with anal canal pathology.

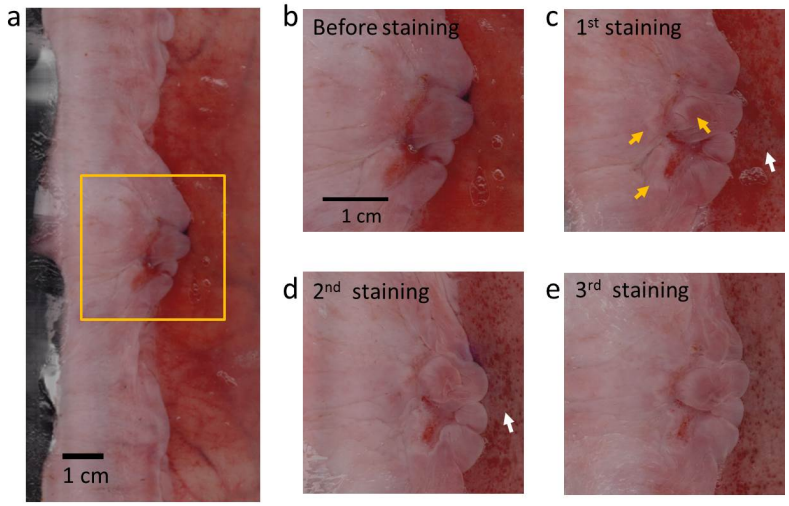

Fig. 5. The time-lapse images of three rounds of acetic acid staining. (a–b) The wide field-of-view (FOV) AnCam image of the anal canal (a) and a zoomed-in region (b) before staining. (c) After the first round of staining, there was a significant whitening of the anal canal epithelium (yellow arrows) and rectum epithelium (white arrow). (d) After the second round of staining, more regions of the anal canal and rectum became whitened. (e) After the third round of staining, the tissue did not become further whitened.

4. Discussion

As a proof of concept, we used an image sensor with 600 dpi (equivalent to a pixel pitch of 42.3 μm) disassembled from a business card scanner, resulting in an imaging resolution of 89 μm. Conventionally, colposcope images are read out either directly from the eyepiece or captured by a CCD video camera, and the resolution of a colposcope is limited by the number of pixels in the camera (the optical resolution is usually much higher). Our current 89-μm resolution is comparable to that of mainstream colposcopes with video cameras using the National Television System Committee (NTSC) standard. For example, these cameras equipped in an Olympus OCS-3 can provide a resolution between 350 μm and 50 μm for magnifications between 3 × and 17 × , respectively.

Recently, up-to-date colposcopes have been shown to be able to provide improved resolution by connecting the scope to a high definition video camera or a digital single-lens reflex (DSLR) camera. For example, the resolution of the LEISEGANG OptiK-2 colposcope with the Canon 600D T3i DSLR camera was measured to be 18 μm at its highest magnification (15 ×). In comparison, the resolution of the AnCam can also be further improved by choosing image sensors with higher pixel densities. As an example, flatbed film scanners such as CanoScan LiDE 700F have 4800 dpi (equivalent to a pixel pitch of 5.2 μm) image sensors, which potentially can improve our resolution to 10 μm.

The cost of our AnCam prototype is less than $150 (not including the computer), which is two orders of magnitude lower than a typical colposcope. The whole AnCam inspection simply includes the insertion of the probe and a quick 10-sec scan, with no refocusing or any extra steps needed, thus, making it very easy to operate. This simplification of the anal canal examination process is highly desirable. In addition, the AnCam can be quite attractive for telemedicine applications whereby diagnoses can be made in low-resource settings where colposcopes are not affordable or specially trained personnel are not available. Under this

#226184 - $15.00 USD Received 6 Nov 2014; revised 19 Jan 2015; accepted 22 Jan 2015; published 27 Jan 2015

circumstance, the AnCam can generate an objectively obtained and digitally stored image containing all of the information from the entire anal canal. This image can then be remotely transferred to specialized centers where experienced professionals can interpret it for the screening of potential anal dysplasia.

It is worth noting that the morphologies of the stained tissue do not appear completely similar in the AnCam images compared with the HRA images, as shown in Fig. 4(d) and 4(f). This is because the tube of the AnCam stretches the pliable mucosa on the transparent polycarbonate tube so that the entire anal canal surface is tightly attached to the tube surface. In comparison, in HRA, the clear plastic anoscope allows the colposcope to visualize the collapsed anal mucosa through its open end. The tissue observed by the colposcope can have folded regions due to the pliable nature of the anal mucosa, thus making it difficult to inspect by HRA. On the other hand, the AnCam potentially has the advantage of observing the details hidden in these folded regions. For this purpose, the tube diameter should be carefully chosen: a too-small diameter may not be sufficient to fully stretch the folded tissues, while a too-large diameter may cause pain or injury to patients. This can be easily addressed by designing AnCams with different tube diameters, so that a personalized tube size can be determined after evaluating the anal dimension for each particular patient. The tube part can also be made disposable to avoid cross-contamination among patients. For our current AnCam prototype, we used a polycarbonate tube fabricated by a plastic extrusion process. This process generates minor line patterns on the tube surface that sometimes can be observed in AnCam images (Fig. 4(e)). This can be further improved by choosing other plastic tubes made by the injection molding process, which can provide better surface quality.

In this study, we also demonstrated the consistency of AnCam images by tracking the dynamics of the acetowhitening process. This revealed the potential of AnCam in longitudinal follow-up of patients with potential anal canal dysplasia or under anal cancer treatment. Similar to the use of annual mammograms to identify new breast cancers, serial digital images of the entire anal canal can be compared when a follow-up is performed for any abnormal changes, so that any dysplasia inside the anal canal can be detected at a very early stage. Due to its simplicity and minimally invasive nature compared with HRA, the AnCam can also be suitable for regular preventive screenings among populations of patients with sexually transmitted diseases or male homosexual contact for the early diagnosis of HPV infection or anal cancer.

5. Conclusion

High resolution anoscopy is the gold standard for the screening of anal dysplasia. Conventional HRA is based on the use of a colposcope. The imaging geometry of the colposcope is ill-matched to the geometry of the anal canal. This results in an imaging procedure that is labor-intensive, time-consuming, and operator-dependent. To address these shortcomings, we designed and built a novel scanning endoscopic system, the AnCam, using CIS technology. The AnCam utilizes low cost and disposable parts, has a resolution of 89 μm, a DOF of 0.65 mm at 5.9 lp/mm, and a maximum FOV of 100 mm × 120 mm. The AnCam can complete a full scan of the anal canal within 10 seconds, a fraction of the time required for a conventional HRA examination (typically more than 30 min), and the images are standardized and reproducible. Lastly, the use of the device does not require specialized training. The overall imaging performance, the reproducibility of the images, and the ease-of-use render the AnCam a highly attractive potential alternative to current imaging modalities of the anal canal and other cylindrically shaped anatomic sites, such as the esophagus.

Acknowledgments

This project is funded by the California Institute of Technology and City of Hope Biomedical Initiative Fund. The authors acknowledge the support by China Scholarship Council and NSFC 61471315.